

Review

Review of Single-Phase Bidirectional Inverter Topologies for Renewable Energy Systems with DC Distribution

Meshari Alshammari ^{1,2}  and Maeve Duffy ^{1,*}

¹ Power Electronics Research Centre, School of Engineering and Ryan Institute, University of Galway, H91 HX31 Galway, Ireland

² Electrical Engineering Department, College of Engineering, Jouf University, Sakaka 72388, Saudi Arabia

* Correspondence: maeve.duffy@universityofgalway.ie

Abstract: Recent developments in renewable energy installations in buildings have highlighted the potential improvement in energy efficiency provided by direct current (DC) distribution over traditional alternating current (AC) distribution. This is explained by the increase in DC load types and energy storage systems such as batteries, while renewable energy sources such as photovoltaics (PVs) produce electricity in DC form. In order to connect a DC distribution system to the alternating current grid (e.g., for backup, delivering energy storage to the grid) there is a need for a bidirectional inverter, which needs to operate over a wide range of source and load conditions and is therefore critical to the overall system performance. However, DC distribution in buildings is relatively new, with much of the research focused on the control of the DC bus connection between sources and loads, rather than on the grid connection. Therefore, this review aims to explore recent developments in bidirectional inverter technologies and the associated challenges imposed on grid-connected DC distribution systems. The focus is on small-scale building applications powered by photovoltaic (PV) installations, which may include energy storage in the form of batteries. An evaluation of existing inverter topologies is presented, focusing on semiconductor technologies, control techniques, and efficiency under variable source and load conditions. Challenges are identified, as are optimal solutions based on available technologies. The work provides a basis for future developments to address current shortcomings so that the full benefits of DC distribution can be achieved.



Citation: Alshammari, M.; Duffy, M. Review of Single-Phase Bidirectional Inverter Topologies for Renewable Energy Systems with DC Distribution. *Energies* **2022**, *15*, 6836. <https://doi.org/10.3390/en15186836>

Academic Editors: Jelena Loncarski and Diego Bellan

Received: 19 August 2022

Accepted: 11 September 2022

Published: 19 September 2022

Publisher's Note: MDPI stays neutral with regard to jurisdictional claims in published maps and institutional affiliations.



Copyright: © 2022 by the authors. Licensee MDPI, Basel, Switzerland. This article is an open access article distributed under the terms and conditions of the Creative Commons Attribution (CC BY) license (<https://creativecommons.org/licenses/by/4.0/>).

1. Introduction

1.1. Background and Motivation

Renewable energy sources, including solar photovoltaics (PVs) and wind turbines, are considered the most dominant solutions to guarantee energy security, with solar PVs outweighing the advantages of other sources in terms of cost and environmental friendliness [1]. However, in order to maximize the supply of energy from renewable sources, the efficiency of the path from source to load needs to be optimized. For instance, the integration of a photovoltaic (PV) system with a conventional alternating current (AC) distribution system requires an inverter to convert the direct current (DC) electricity produced by PVs into a standard AC grid form. On the other hand, there is an ever-increasing range of domestic appliances and equipment that operate from a DC supply, e.g., computing and audiovisual equipment, cordless vacuum cleaners, etc., but they require an AC/DC rectifier stage to connect to the conventional AC distribution system (mains). In recognition of the improved efficiency provided by DC distribution between a DC source and DC loads (through the elimination of two complementary stages of power conversion), there has been significant growth in the range of appliances configured for supply from a DC distribution system, e.g., cooling, heating, lighting, refrigerator, washing machines,

etc. [2]. Indeed, standards are being developed for DC-configured products under the EMerge Alliance [3], in which a high DC voltage level of 300–380 V is preferred in terms of distribution capability, lower equipment cost, and simplicity of integration with existing system infrastructure [4]. It is worth mentioning that such DC appliances correspond to over 60% of the total electricity consumption of householders in the U.S. [5].

In order to determine the benefit provided by DC distribution, recent studies have analyzed the relative efficiency of AC and DC systems [6,7]. Increased efficiency of up to 16% has been predicted for DC vs. AC when a PV installation and energy storage are utilized. A similar level of improvement was reported in [8] in which an additional energy source, such as a gas engine, was included with PVs, providing increased efficiency of 15%. Even in the absence of a PV source, in [9], the application of a DC distribution system in an office building was predicted to have lower power losses by up to 14.9% compared to the AC systems when only powered by the grid energy. In the case where renewable energy and energy storage are integrated with the utility grid through DC, optimal efficiency of up to 50% has been predicted for small-scale buildings [10,11]. This is encouraging for residential buildings which are likely to achieve self-sustainability compared to commercial buildings [10], thereby achieving the advantages of net-zero energy, such as resilience and reliability, and sustainability in buildings can be optimized.

However, when a DC distribution system is implemented and integrated with the AC grid, an inverter with bidirectional power flow is usually needed to feed the grid in the case of excess power from the PVs and to supply power from the grid to maintain the DC bus at a nominal voltage when the load demand is higher than PV generation. This compares with standard unidirectional inverters, which are normally used to feed PV energy into an AC distribution system. Bidirectional inverters have been widely used in higher power applications such as energy storage batteries and plug-in hybrid or fully electric vehicles. In electric vehicle (EV) applications, the bidirectional capability may be required to facilitate vehicle-to-grid (V2G) between the grid and the DC bus, although normally, only a unidirectional rectification stage is used to charge the EV battery. However, since EV battery charging has its own specific requirements in terms of battery voltage and charging algorithms, it is not considered further. Instead, this work concentrates on the bidirectional inverters in DC distribution systems integrated into residential buildings.

Despite their importance, the design and implementation of bidirectional inverters for DC distribution in buildings are relatively immature. As a result, there are several approaches described in the literature, but they have not been widely compared or assessed. This review takes the opportunity to address this gap so as to advance the understanding of the impact of bidirectional inverters in DC distribution systems, while also identifying technical challenges to be addressed in future research. The results will lead to the development of more efficient DC distribution systems towards enabling net-zero buildings, as predicted in the studies above.

1.2. Bidirectional Inverter Challenges

The interface between the DC bus and the AC grid is crucial because it can reduce the operation efficiency and stability of the overall system performance. Therefore, methods for increasing the efficiency of bidirectional inverters have received considerable attention because they relate to the return on investment of the DC system. High efficiency over a wide range of power levels has significant benefits for increasing DC system efficiency in buildings, especially small-scale domestic installations, where there is usually a mismatch between periods of PV production and energy consumption [12–14]. This is less relevant for commercial buildings.

Transformerless topologies are widely used to reduce losses (and costs) associated with transformers in isolated topologies. However, it is important to highlight that due to dynamic coupling between the shared AC and DC ground in a transformerless solution, the parasitic capacitance of PV panels causes a leakage current. This has a negative impact on the inverter efficiency and needs to be minimized to avoid significant loss [15]. The effect

varies depending on the common mode voltage (CMV) across the parasitic capacitor, and therefore, modulation strategies can alleviate the issue [16]. Other solutions are discussed in more detail below.

High leakage current may lead to the additional distortion of the output grid current caused by high-frequency operation, where the utility grid standardization needs to be in compliance with the safety regulations of electrical equipment. On account of this, an EMI filter is required to attenuate the grid current to an optimal level of quality on the AC side in the case of inverter mode. However, while the ground of the AC and DC sides are shared through the distribution plant in the building, the common-mode (CM) and electromagnetic interference (EMI) noise-related issues will cause an impact on the DC side. The DC-bus voltage, as well as differential-mode (DM) and (CM) noise, must be kept within a small-voltage ripple to provide improved power quality, ensure reliable load operation, and reduce significant loss in the system. Different filtering schemes to address this are described later. It is shown that the additional number of passive components, as well as the complexity of the associated control approach, would reduce the efficiency of the design. As a consequence, a trade-off must be made in the development of a suitable EMI filter in order to reduce the aforementioned concerns.

Given the strong correlation between the leakage current and the EMI filter, it should be noted that the range of current that the filter inductor needs to support is another challenge due to the potential nonlinear characteristic of its core material. As a result, the tracking accuracy of the employed current controller to set the required grid current may be influenced by the inductor current ripple. Moreover, errors in zero-crossing detection for grid synchronization could be introduced due to insufficient magnetization of the inductor core material which has an impact on the grid current. This effect is important for both inversion and rectification modes in a grid-connected inverter. Indeed, in rectification mode, power factor correction (PFC) is required to reduce the consumers' load demand for reactive power. In addition, the harmonic regulation has to be fulfilled according to the required grid code. It is worth noting that the response to different weather conditions of renewable energy sources such as PVs can cause a wide voltage variation on the DC side of the bidirectional inverter. Under this circumstance, the authors of [17] offer buck/boost maximum power point tracking (MPPT) to mitigate the sudden change of voltage and associated stress applied to the DC bus interfaced with a grid-connected inverter. This is important to ensure that the bidirectional inverter supplies local load conditions as well as to the grid, efficiently and reliably. The power flow of the bidirectional inverter needs to be maintained based on the DC-bus voltage when subjected to variable source and load conditions [18]. The control capability also has to assure the stability of the entire system when subjected to a certain level of load demand due to shared power supply either from renewable energy or the grid. Moreover, the DC bus needs to be regulated at a nominal voltage to enable the operation of the battery charge controller and a reliable supply of DC system. On the other hand, the power delivered by the DC-bus in case of excess power from PVs has to meet the standard power regulations of the grid [19,20].

In addition to maintaining stable DC and AC voltage levels and grid synchronization [21,22], the DC-side interaction with the AC grid must be decoupled and isolated in the case of a fault or potential transient which can affect the dynamic operation of the system [23]. Furthermore, the phase shift during the transition period between inversion and rectification modes should not affect the DC system's reliability. Considering that certain bidirectional inverter types have two stages of power conversion, the control structure may become more complex if the transition between modes is performed effectively to achieve high performance levels. The control design of the DC-bus interface with renewable energy is discussed in more detail in Section 5.

1.3. Paper Structure

The paper consists of five sections. A brief overview of DC distribution system configurations involving a bidirectional inverter is presented in Section 2. Section 3 begins by

laying out the historical overview and theoretical implementation of bidirectional inverter topologies and looks at how they are controlled with the utility grid. Section 4 presents a comparison of the performance between different topologies to highlight the optimal design. Section 5 presents a comparison and classification of the various techniques and parameters used in different control systems for bidirectional inverters. Finally, a conclusion summary is given in Section 6, which includes challenges and limitations associated with the bidirectional inverter and suggestions to be considered for future implementation.

2. DC Distribution System Configurations

With the development of efficient DC distribution systems in buildings in recent years, it has commonly been assumed that the combination of different energy sources could enhance performance. However, it has been shown that the DC system performance could vary in terms of efficiency depending on load profile, utilized renewable energy sources, and utility grid integration [10]. Figure 1 illustrates a general schematic configuration of DC distribution systems in buildings, including renewable energy sources (PV in this case), energy storage, and a mix of AC and DC loads [24–27]. The system contains a power optimizer known as a maximum power point tracking (MPPT) to maximize the PV output power under different weather conditions [28]. In addition, a step-up/down DC/DC power converter is implemented for charging/discharging the energy storage and to control the power flow to regulate the voltage level of the DC bus.

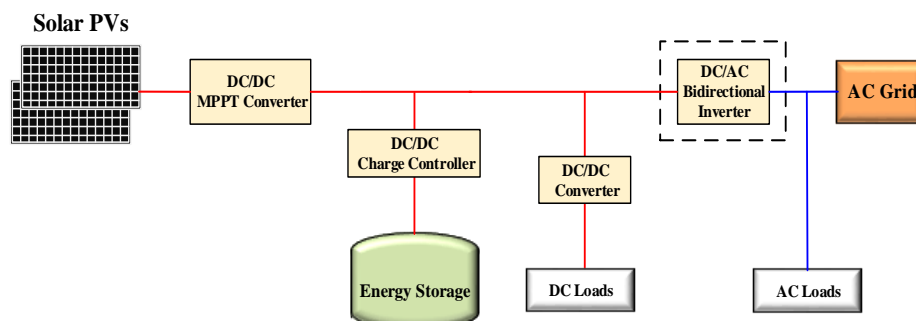


Figure 1. Schematic configuration of DC distribution systems integrated with a grid and a backup system.

The integration of grid power is required to assure the continuous operation of the system in supplying the DC loads in the case of insufficient power, either from renewable energy sources or energy storage. However, there are some configurations of DC systems that do not employ renewable energy sources, in which energy storage and/or a fossil fuel-based generator and grid power are utilized instead. Under these circumstances, energy storage could be beneficial to address the peak saving and ensure the security of supply, or for applying demand-side management when there are no alternative energy sources. On the other hand, regardless of the importance of energy storage, it is not always included in DC system configurations.

Despite the progress and optimal efficiency of DC distribution system implementation, there is still no consensus on standardization and regulation. The EMerge Alliance has developed a standard for 24 Vdc distribution for low power loads within inhabited areas, and several certified infrastructure solutions have successfully shown compliance with this standard [2]. However, 24 V is not compatible with typical battery and inverter voltages. In addition, the alliance has recommended the implementation of a 380 Vdc standard for use in higher power applications such as data centers and central telecom offices [2]. This standard might pave the way for DC distribution in residential and commercial applications at voltages greater than 24 V, which would be advantageous for both sectors. As a result, the academic literature on such systems integrated into buildings has revealed the emergence of several contrasting themes in terms of DC bus configuration and voltage level [29–31]. The purpose of a DC-distribution system is to eliminate some of the integrated conversion

stages to increase the overall distribution system efficiency. However, depending on the range of loads to be supplied, there are two dominating DC bus structures, bipolar and unipolar, as presented in Figure 2. The principle of a bipolar type is that the DC bus has three lines, positive and negative lines, $+V_{dc}$, $-V_{dc}$, and the middle line is a neutral line [32–34], to allow the supply of loads with two available voltage ranges, as depicted in Figure 2a. In addition, the system has robust reliability to guarantee that loads are fed when an electrical fault occurs in either line [35]. Moreover, with a bipolar structure, the neutral point is grounded, which considerably reduces the line-to-ground safety risk by significantly reducing the highest allowable DC-line voltage relative to the ground.

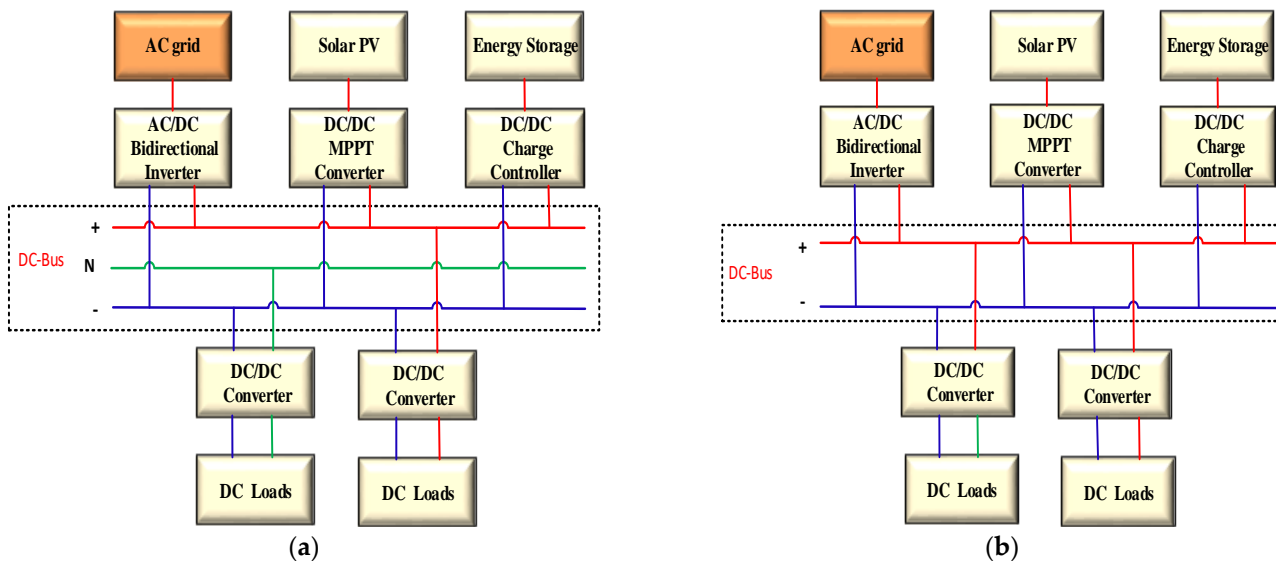


Figure 2. The structure of (a) bipolar DC bus, (b) unipolar DC bus.

Figure 2b shows the unipolar DC distribution system with one consistent voltage level, represented by the use of two lines, one labeled “ $+V_{dc}$ ” and the other “ $-V_{dc}$ ”. The unipolar structure is more suitable for systems with low power loads due to the cost saving associated with reduced wiring compared to the bipolar type [36]. However, the lower voltage level of unipolar systems may limit the efficiency that can be achieved regardless of its cost benefits [37]. In terms of these DC bus structures integrating with the grid through a bidirectional inverter, there is one study implemented with a bipolar type (Figure 2a) [38]. This approach usually experiences additional costs in terms of control structure and computation, and ultimately the overall benefit is slightly higher when unipolar is used.

A comparison of the existing empirical literature on DC-bus voltage versus power integrated with a single-phase bidirectional inverter is illustrated in Figure 3. Based on the results, it may be observed that once the power level is high, the voltage typically corresponds to that of the peak mains, i.e., $\sqrt{2}$ times the root mean square (rms) voltage. It can be seen that the majority of the DC bus voltage levels fall somewhere in the region of 380 to 400 V. High-voltage operation (i.e., 600 V) is applied in cases where two voltage levels (600 V/300 V) may be required, allowing for the adaptability of DC load connection. Nevertheless, it is possible to conclude that the high power and voltage level (i.e., 10 kW and 600 V) is not appropriate for residential buildings from a safety perspective, despite the fact that it provides a high level of efficiency.

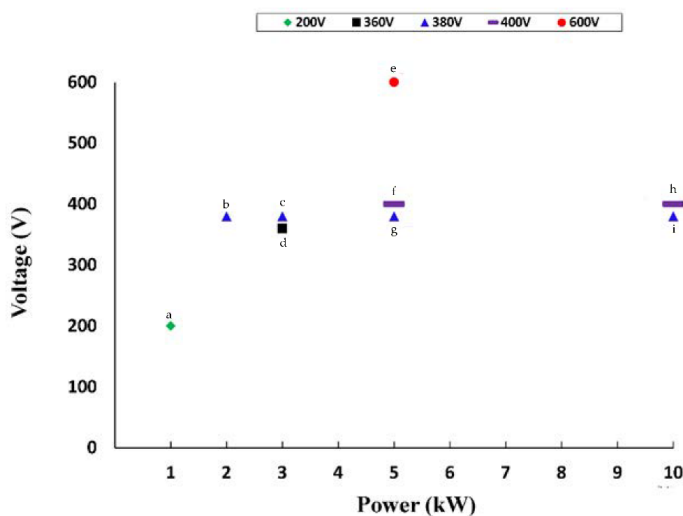


Figure 3. DC-bus voltage level integrated with a bidirectional inverter. a—[39,40]; b—[41]; c—[42]; d—[43]; e—[44]; f—[45–50]; g—[51–55]; h—[38,56,57]; i—[58].

3. Single-Phase Bidirectional Inverter Topologies

Single-phase inverters are generally classified into two types: voltage source (VS) and current source (CS) inverters. The VS inverter is widely used for PV grid-connected applications due to its advantages of high efficiency, economical cost, and the size of implementation [59,60]. It provides a good solution when the required voltage needs to be maintained regardless of the current variation. Meanwhile, the CS inverter is usually used in applications involved in controlling the torque, such as electrical vehicles (EVs), where the current needs to be controlled. This paper is mostly concerned with VS inverters.

Traditional inverters have unidirectional power flow, while in a DC distribution system, a bidirectional power flow interfaced between the DC bus and utility grid is usually required. A summary of the existing implemented bidirectional topologies used in DC distribution systems in buildings is illustrated in Figure 4. These may be categorized into transformer and transformerless inverters/converters. In turn, the transformerless topology can be grouped into four sub-groups based on their functionality of (a) voltage stress and decoupling between the DC and AC sides, i.e., common ground; (b) H-bridge; (c) H6; and (d) two-stage non-isolated topology [61,62]. In order to shed more light on each topology considering the main concerning factors such as leakage current (I_{cm}) and common mode voltage (CMV), the following sections provide an analysis of the topologies utilized, illustrating the efficiency and control challenges and optimal design aspects.

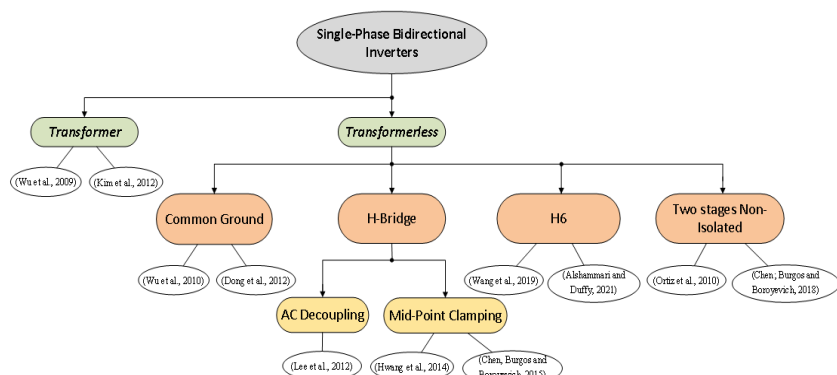


Figure 4. Classification of single-phase bidirectional inverter topologies integrated with a DC distribution system. (We et al., 2009)—[63]; (Kim et al., 2012)—[51]; (Wu et al., 2010)—[52]; (Dong et al., 2012)—[44]; (Lee et al., 2012)—[43]; (Hwang et al., 2014)—[39]; (Chen, Burgos and Bonyewich, 2015)

Boroyevich, 2015)—[56]; (Wang et al., 2019)—[53]; (Alshammari and Duffy, 2021)—[54]; (Ortiz et al., 2010)—[64]; (Chen, Burgos and Boroyevich, 2018)—[57].

3.1. Transformer Topologies

To overcome the potential effects of leakage current caused by parasitic capacitance between the PVs and the ground of the utility grid, a transformer may be used to provide galvanic isolation [65]. However, if operating at the mains/line frequency (LF), a large transformer size is needed to prevent saturation in the core, and that could decrease the efficiency and introduce further weight and cost to the system [66]. An alternative method is to resort to a high-frequency (HF) transformer to reduce the transformer size. However, this could lead to an increase in power loss and requires a relatively high level of system complexity, especially when integrating DC distribution systems, as the bidirectional power flow and regulation of the DC bus are required to be balanced when multiple power sources are applied, in addition to the bus being subjected to different load conditions.

The study of [63] has provided details on the adaption of the push-pull isolated topology for low-voltage DC bidirectional inverters integrated into the grid as shown in Figure 5a. This topology provides the ability to step up or down, which is important in applications where the DC bus voltage level is less than the peak mains. However, the topology needs to be operated at a relatively high frequency (20 kHz) to ensure that the transformer size is reasonable, and this limits its efficiency to some extent. The push-pull also provides the function of PFC in the case of the rectification mode, while using phase-shift control in the inversion mode. A notable feature of this topology is the benefit of a low number of switches and associated driver circuitry, which can avoid additional power losses compared to other transformer-based bidirectional inverters [67]. However, it seems that the current harmonic in PFC mode is relatively high when the system is operated for a wide range of power levels (1 kW to 5 kW in this case). Similarly, for the inversion mode, a high current harmonic distortion is introduced when the load demand is higher than 1 kW.

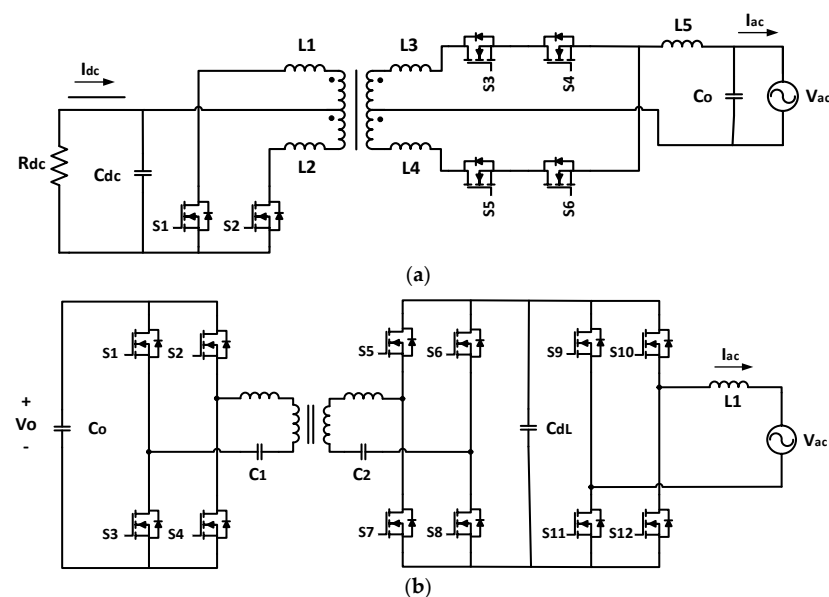


Figure 5. Illustration of bidirectional transformer topologies: (a) push-pull topology [63] and (b) isolated bidirectional boost rectifier AC–DC converter [51].

In recognition of their superior performance and efficiency, significant research on the application of DC/DC topologies to isolated bidirectional converters has recently been published [68]. Thus far, the development of a high-power isolated full-bridge boost rectifier with bidirectional capability is proposed [69]. However, as with all transformer-based solutions, leakage inductance causes high current spikes during switching and significant effort has been directed at addressing this through snubber circuits. Using an

RCD passive snubber to clamp the voltage is the most straightforward method; however, the resistor dissipation adds to power loss, resulting in low efficiency. Alternatively, active and passive clamping circuits may reduce voltage stress caused by the leakage inductance of current-fed inductors and isolation transformers [69]. However, due to the existing resonant current of the capacitor in some clamped circuits, the current stress on the switches is significantly increased, resulting in higher power loss and a corresponding decrease in efficiency. Therefore, a flyback snubber provided by the authors of [70] is used to recycle the energy that the clamping capacitor absorbs. Moreover, the clamping capacitor voltage can be controlled autonomously by the flyback snubber. The characteristic of zero-voltage transition (ZVT) was applied to a phase-shift full bridge at high frequency to achieve high efficiency for bidirectional capability [71]. The topology maintains a constant output voltage by decreasing the input voltage, which usually varies.

The bidirectional operation of an LLC resonant converter is introduced in [72] and has the ability to reduce the switches' voltage stress without any snubber circuitry. However, it is possible that the wide operating range of the converter necessitates a compromise between the turn ratio of the transformer and the utilization of the resonant characteristics. Therefore, a high-efficiency isolated bidirectional inverter with two stages of power conversion was proposed by [51] to overcome the high switch conduction loss of the bidirectional boost rectifier, as shown in Figure 5b. However, the overall efficiency of this topology tends to be low at light loads.

3.2. Transformerless Topologies

The full-bridge (H4) transformerless topology, as shown in Figure 6a, is most commonly used for bidirectional conversion in renewable energy applications, e.g., [52]. Since there is no transformer, it generally provides a smaller solution, and the issue of transformer leakage current is eliminated. However, it has its own issues. The fluctuation of filter inductance due to non-linear core material properties over a wide current range causes current oscillation and significant current ripple, lowering current tracking accuracy [52]. As a consequence, the DC-bus and grid voltages will vary. In order to reduce this fluctuation in a single cycle, a closed-loop control system was designed that attenuated the required duty cycle to provide the desired inductor current while also reducing variations in the DC-bus and grid voltage. However, the efficiency of this topology is low.

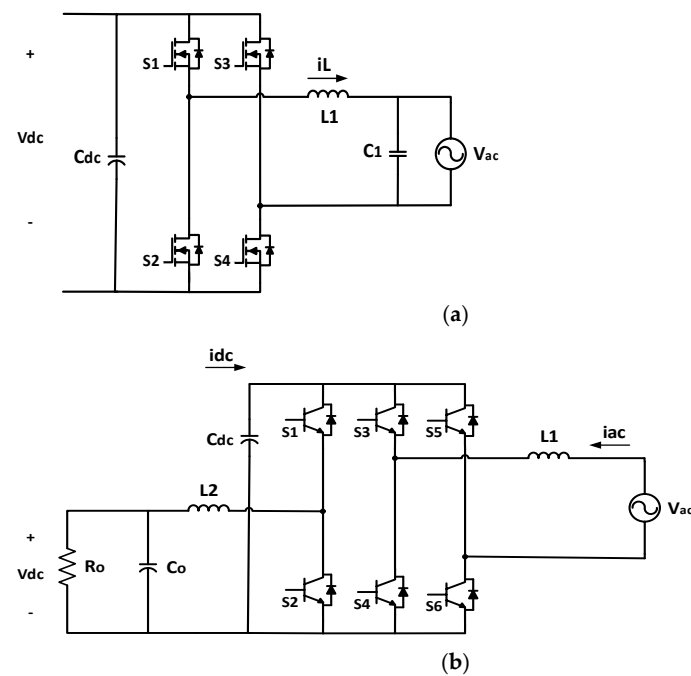


Figure 6. Bidirectional inverter (a) conventional H4 [52] and (b) two-stage topology [64].

To address the challenge of maintaining a stable DC bus voltage under transient load conditions, the work of [64] offered an improvement in which the stability of the DC-bus voltage is maintained and the DC-link capacitor is reduced by using a two-stage power conversion scheme where the H4 is employed in series with a DC/DC stage as shown in Figure 6b. As can be seen, the DC/DC acts as a buck during rectification and as a boost during inversion.

A modified H4 topology with an EMI filter connected to the grid is proposed in [44], as shown in Figure 7. The topology aims at reducing the leakage current on the DC side caused by high-frequency unipolar PWM on the AC side. It includes an output LCL filter with a common-mode choke in which the neutral point is connected directly to the mid-point of the DC link. This involves a split-phase DC line employing two extra DC capacitors. Consequently, this AC filter structure could add additional power loss, which limits efficiency. Therefore, there is a trade-off between CMV on the DC side and high efficiency, in which case the overall system performance, particularly at low consumption power, could be improved.

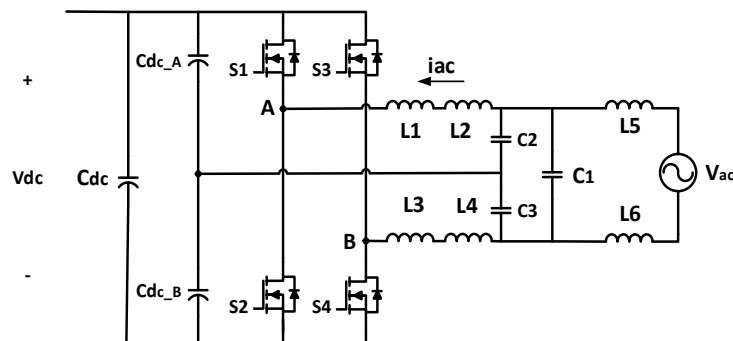


Figure 7. Modified H4 bidirectional full-bridge topology with EMI structure [44].

Another issue with the H4 topology is that it, too, suffers from power loss due to leakage current through the parasitic capacitance of the PVs [73]. In order to overcome this effect, the authors of [43] propose a solution that provides two additional current paths on the AC side, where the inverter output is driven into three levels of VAB (V_{dc} , 0, and $-V_{dc}$), as depicted in Figure 8. Since the rate of change in voltage across the parasitic capacitance (ground capacitor) is reduced, this design can limit high-frequency components and reduce leakage current. As a result, the inductor loss during freewheeling is reduced, while injected reactive power from the grid is reduced in the case of zero crossing. Due to the fact that the topology operates as a boost in rectification mode, the DC-link voltage limitation is required to be nearly twice as high as the power grid's peak voltage. However, there is no capacitor connected to the AC terminals, which impacts the EMI performance. High efficiency was achieved in this case but is partly owing to the use of oversized semiconductor devices relative to the design specification.

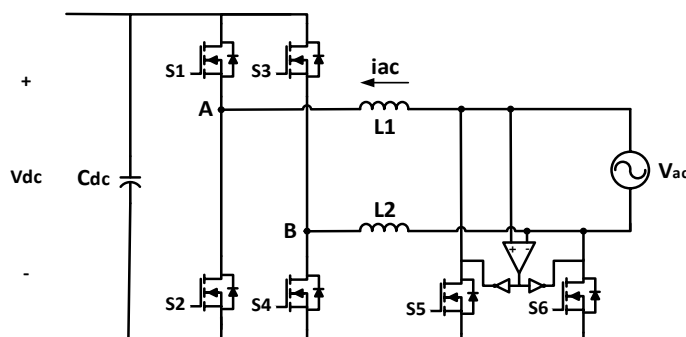


Figure 8. H4 bidirectional inverter full-bridge topology with additional paths [43].

Loss analysis of the H4 topology found that high losses are contributed by large inductor current ripple, in addition to the loss of the switches operating at high frequency [39]. Therefore, an interleaved three-leg full-bridge inverter was proposed as shown in Figure 9 in which high and low switching frequencies are applied for the middle and outer legs, respectively, where a predictive control strategy was implemented to synchronize the grid voltage and current. However, leakage current still presents a challenge in which the flow of current during different parts of the cycle is discontinuous. No details of the efficiency were provided in this case.

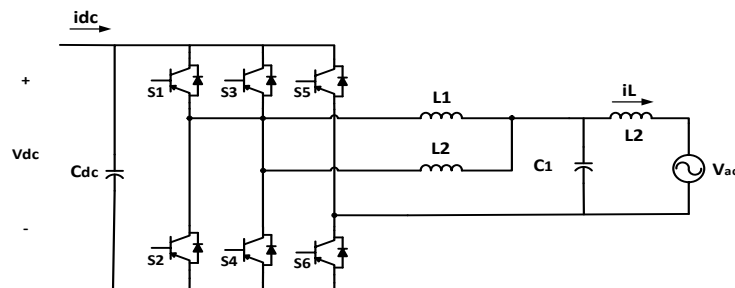


Figure 9. Interleaved single-phase three-leg of full bridge topology [39].

The study of [56] offers probably one of the most comprehensive empirical analyses of the transformerless H4 topology when employed in a two-stage interface between the grid and DC sources. The authors present an analytical loss breakdown for the H4 and propose a method for minimizing losses caused by the EMI and CM filters. Figure 10 shows the proposed 2-level (2L) full bridge with LCL filter in (a), while a parallel version is proposed in (b). The efficiency was highest when the 2L parallel structure was employed due to the reduction in conduction losses provided by paralleling and the use of SiC MOSFETs for decreasing the switching losses. Similarly, an emphasis on the performance of semiconductors device such as SiC MOSFET provides potential performance for enhancing the bidirectional inverter efficiency compared to ideal MOSFETs and IGBTs [41]. However, this topology does not address the issue of capacitive leakage current and associated CMV.

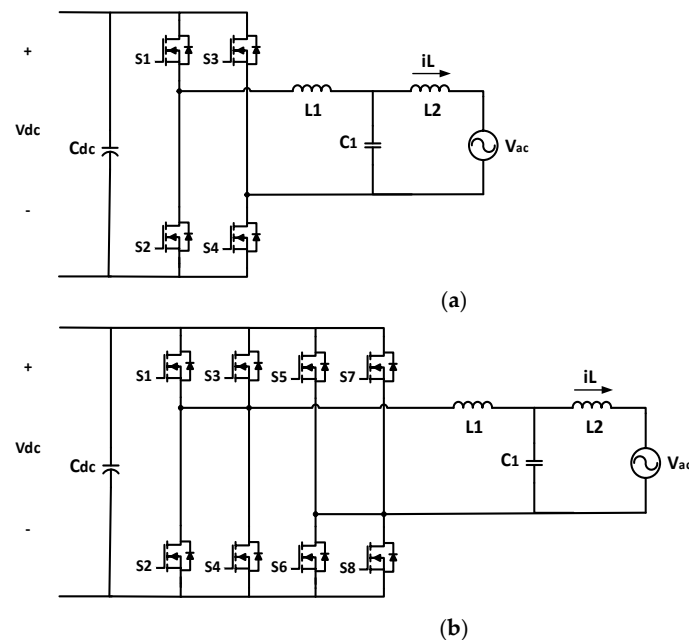


Figure 10. Bidirectional inverter topologies of (a) a 2L full bridge with LCL filter, (b) a 2L parallel full bridge [56].

Since solutions to the leakage current and associated CMV may require additional components and increase the cost and size of the bidirectional inverter, a new H6 transformerless inverter topology was proposed (firstly as a unidirectional inverter) in [74] that eliminates the leakage current, reduces the inductor harmonics current, and prevents the voltage spikes that occur in inductive loads. During the inductor free-wheeling interval in the positive half-cycle, the current flows through D1 and diode S5. This not only disconnects the DC side from the grid but also prevents the high-frequency voltage from building up in the parasitic capacitance, which lowers the leakage current. The same is applicable for the path through S6 and D2 during the negative half-cycle of the grid. Furthermore, its efficiency was improved in [75] with a modified PWM pattern when there is a phase shift between output current and voltage. Therefore, these features of the H6 outweigh other unidirectional transformerless topologies such as the H5, HERIC, etc.

The H6 was modified to operate with the capability of bidirectional power flow in [53], as shown in Figure 11a. However, it is indicated that under light load conditions (roughly 1.2 kW for a 5-kW rated system), a reduction in inverter efficiency was observed. This study also confirms that switches of the inverter could play an important role to maximize the overall efficiency. Therefore, a study of [54] proposed the synchronous H6 topology, as can be seen in Figure 11b, to reduce the greatest impact of the diode conduction loss and its related switching ON losses under full loads. Similarly, these dominant losses were reduced under rectification mode by using SiC MOSFETs instead of diodes D1 and D2.

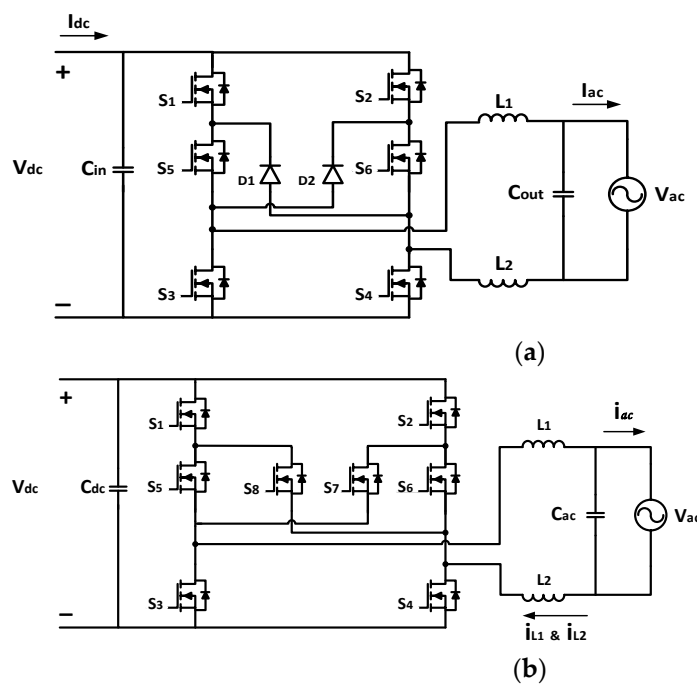


Figure 11. H6 bidirectional inverter topology: (a) standard H6 [53] and (b) synchronous H6 [54].

A small number of papers discuss bidirectional inverters for a bipolar DC configuration, in which the DC and low-frequency CM voltages need to be closely regulated to ensure symmetrical DC bus voltages and to reduce leakage current. The high-frequency CM noise can be filtered out by passive components, as with unipolar DC systems [23]. The authors of [76] proposed a control solution for grounded unidirectional inverter systems with power converters, which is based on an active common-mode duty cycle injection approach. As a result, a reduction in voltage ripple was achieved, which minimized the ground leakage current. However, this control technique does not apply to bidirectional operation. Therefore, the topology proposed in [57] and presented in Figure 12 was designed for enabling bidirectional capability and high frequency. Moreover, the leakage current was reduced due to the decoupling of the CM voltage, while the high-frequency

noise was eliminated by the filter. Moreover, an interleaved schematic of this topology was introduced to mitigate the inductor choke ripple, which may lead to an additional loss, resulting in low efficiency in both stages. Furthermore, this topology requires extra switching devices and passive components to enable the converter to transition between the inverter and rectifier operation while maintaining DC-bus voltage. In addition, when the active damping method is implemented, the need for extra voltage and current sensors increases the overall cost of the system. Therefore, it is feasible that an alternative solution may be established to perhaps reduce the cost and size of the converter with respect to its level of efficiency.

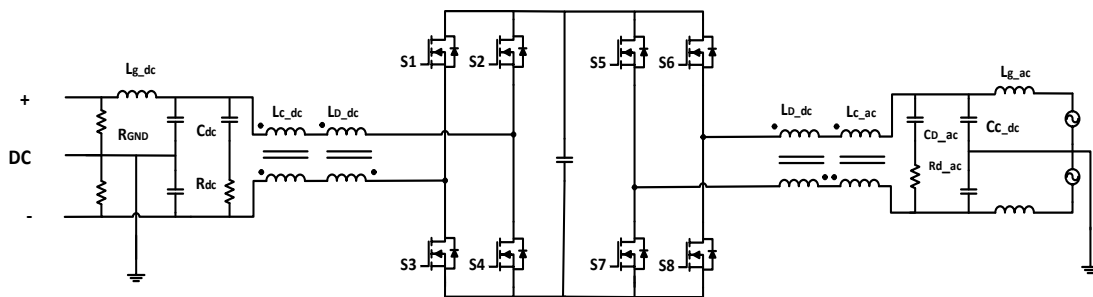


Figure 12. Two-stage bidirectional converter with CM decoupling [57].

4. Performance and Evaluation

The bidirectional inverter topologies considered in Section 3 are summarized and compared in this section. Table 1 compares the topologies in terms of controller implementation, switching frequency, and output filter.

Table 1. Control modulation and passive devices of transformer and transformerless bidirectional topologies for DC distribution systems.

| Ref. | Topology | Power Level (W) | SPWM/Implementation | Switching Frequency | Filter/EMI | DC-Bus Voltage | DC Link Capacitor | Line Voltage |
|---------|--|-----------------|--|-----------------------|--------------|----------------|-------------------|----------------|
| [63] | Push-pull phase-shifted—transformer | 600 | DsPIC30F2020 at dc side Cycle converted at the ac side bipolar | 20 kHz | LC | - | Non | 50 Vac/120 Hz |
| [52,77] | Full-bridge bidirectional inverter transformerless | 5000 | DsPIC30F2023 | 20 kHz | LC | 340–380 | 3760 F | 220 Vac/60 Hz |
| [45] | Full-bridge bidirectional inverter transformerless | 5000 | TMS320LF2406A | 20 kHz IGBT | LCL | 360–400 | 560 F × 10 | 220 Vrms/60 Hz |
| [78] | Full-bridge bidirectional inverter transformerless | - | DsPIC30F2023 | IGBT | LC | - | - | - |
| [46] | Full-bridge bidirectional inverter transformerless | 5000 | TMS320LF2406A Bipolar/Unipolar | 20 kHz IGBT | LC | 360–400 | 560 F × 10 | 220 Vrms/60 Hz |
| [47] | Full-bridge bidirectional inverter transformerless | 5000 | TMS320LF2406A | IGBT | LC | 360–400 | - | - |
| [44] | Full-bridge bidirectional inverter transformerless | 10,000 | PWM Unipolar | 20 kHz IGBT | parallel LCL | 600 | 360 F | 240 Vrms/60 Hz |
| [55] | AC–DC boost bidirectional rectifier | 5000 | TMS320F28335 Unipolar | 13.8 kHz MOSFETs IGBT | LPF | 380 | 2.7 mF | 220 Vac/60 Hz |
| [51] | Full-bridge CLLC resonant bidirectional converter | 5000 | TMS320F28335 PFM | 58–65 kHz MOSFETs | FIR | 380 | 200 nF | 220 Vac/60 Hz |
| [43] | Full-bridge bidirectional inverter transformerless | 3000 | PI | 16 kHz MOSFETs | parallel L | 360 | 2200 μF | 220 Vrms/60 Hz |

Table 1. Cont.

| Ref. | Topology | Power Level (W) | SPWM/Implementation | Switching Frequency | Filter/EMI | DC-Bus Voltage | DC Link Capacitor | Line Voltage |
|---------|---|-----------------|-----------------------------------|---------------------|--------------|----------------|---------------------------|----------------|
| [48] | Full-bridge bidirectional inverter transformerless | 5000 | D- Σ digital PWM rectifier | 20 kHz IGBT | LCL | 360–400 | - | 220 Vrms/60 Hz |
| [79] | Bidirectional transformerless PV inverter based on HFLs | 8000 | Phase-shift | 50 kHz IGBT MOSFETs | LC | 380 | $6 \times 1.0 \text{ mF}$ | 220 Vrms/50 Hz |
| [38,57] | Two-stage bidirectional AC–DC converter | 10,000 | Pluggable phase-leg module | 40 kHz MOSFETs | DM | 380 bipolar | 100 nF | 240 Vrms/60 Hz |
| [41] | Two-stage bidirectional AC–DC converter—NPC and FB | 2000 | Unipolar | 20 kHz MOSFETs IGBT | LCL | 380 | - | 127 Vrms/60 Hz |
| [53] | H6 bidirectional transformerless inverter with bridgeless PFC rectifier | 5000 | Unipolar | 20 kHz MOSFETs | parallel L&C | 380 | - | 220 Vac/50 Hz |

What is notable is that digital rather than analog control is most commonly used. This is due to the better control precision and dynamic reactions of digital compared to analog implementations. According to Table 1, unipolar PWM is used for the majority of bidirectional inverters. Given the fact that unipolar leads to lower DC current ripple, it is possible to minimize the AC-side harmonics by a substantial amount in comparison to bipolar PWM. Using unipolar outperforms bipolar, which requires a large inductor to minimize current ripple due to the voltage peak value. However, PWM schemes create a high leakage current at a high frequency on the DC side that flows to the ground in transformerless topologies because of the different switching transitions and dead-times. Consequently, when high-efficiency operation is needed, it is critical to take this into consideration.

Almost all bidirectional inverter topologies were operated at 20 kHz due to the good trade-off between the inductor loss and switching loss of the employed semiconductor devices. Among these are SiC MOSFETs, which have a lower switching loss compared to Si MOSFETs. Conduction loss is a significant issue for IGBT switches, and they are not recommended for use in these bidirectional inverter topologies.

Another trend that is evident in Table 1 is the fact that LC and LCL filters are most common in transformerless topologies, which implies that the inductor design may contribute to minimizing the converter power loss. However, current distortion may occur at low power levels due to the impact of continuous inductor current flow, which may increase conduction loss and reduce overall efficiency.

The majority of bidirectional converter topologies have a power rating of 5 kW, indicating that they can be used in both commercial and residential buildings. While it is true that residential buildings are typically operated at a lower power level, this results in low efficiency for most topologies that are used.

A summary of semiconductor parameters implemented in the bidirectional topologies considered is given in Table 2. In terms of the technologies used, it was noticed that Si MOSFETs and IGBTs were the first to be developed, indicating that they were the primary switching devices available during this period of time. Indeed, such technology, particularly IGBT switches, is suitable for high voltage operation, which explains why they are the mainstream switches. However, as a result of advancements in semiconductor technology, SiC MOSFETs are capable of operating at higher voltages while also delivering higher efficiency when compared to Si MOSFETs and IGBTs. Moreover, because the cost of SiC MOSFETs is high, it is necessary to consider a trade-off between high efficiency and cost when designing a bidirectional inverter. Similarly, the diode used in some topologies, such as those in which the ideal Schottky diode can be replaced by an SiC Schottky diode due to its low power dissipation, can be justified in the same way.

Table 2. Semiconductor components of transformer and transformerless bidirectional topologies for DC distribution systems.

| Ref. | Year of Publication | Device Type | Device Model | Manufacture | V Rated | I Rated | Diode Type | Diode Model |
|---------------|------------------------|--------------|--------------|-------------------------|---------|---------|--------------------|-------------|
| [45,46,49,52] | 2010, 2011, 2012, 2016 | IGBT | 40N60A4 | Fairchild Semiconductor | 600 V | 75 A | Ultrafast | RURG5060 |
| [51] | 2013 | MOSFETs | IXKR47N60C5 | Littelfuse | 600 V | 75 A | - | - |
| | | MOSFETs | SPW47N60CFD | Infineon | 600 V | 75 A | Schottky | C3D20060D |
| [43] | 2014 | Cool MOSFETs | FCA 75N60N | IXYS Corporation | 600 V | 47 A | C3D20060D | |
| | | IGBT | IGW75N60T | Infineon | 600 V | 46 A | | |
| [48] | 2014 | IGBT | G40N60A4 | Gree | 600 V | 75 A | Schottky | C3D20060D |
| [38,57] | 2017, 2019 | SiC MOSFET | C2M0025120D | Wolfspeed | 1200 V | 90 A | - | - |
| [53] | 2019 | SiC MOSFET | C3M0120090D | Gree | 900 V | 23 A | SiC Schottky diode | CVFD20065A |

The relative advantages and disadvantages of the different topologies are compared in Table 3. As compared to other transformerless topologies, the H6 topology claims to provide a high level of efficiency to support the premise that leakage current and high current distortion are kept to a minimum.

Table 3. Main comparison summary of bidirectional single-phase inverters for integration with DC distribution systems.

| Ref. | Topology | Advantages | Disadvantages | Inverter Size | Maximum Efficiency | No. Conversion Stages | Leakage Current | Control Strategy |
|---------|------------------------------------|--|--|---------------|--------------------|-----------------------|-----------------|------------------|
| [63] | Push-pull transformer based | Low DC voltage ripple | High THD Hard switching increase loss | Large | 89% | 2 | High | Simple |
| [51,55] | Isolated AC/DC converter | No CM effect | High level of complexity | Large | 96% | 2 | High | Complex |
| [52,77] | Full-bridge | Small filter. Inductor variation minimized | High THD Voltage and current drop due to inductance change | Small | 97.2% | 1 | Medium | Complex |
| [43] | Modified full-bridge | Low THD | Oversized switches High output voltage and current ripple | Medium | 98.6% | 1 | Low | Medium |
| [39] | Interleaved three-leg full-bridge | Low switching loss | Medium THD due to inductor current ripple in respect invert size Expected CM fluctuation | Medium | - | 1 | High | Medium |
| [56] | 2L full-bridge with paralleled SiC | Small filter | High conduction loss Increased switching loss as frequency increases | Small | 93% | 1 | High | Medium |

Table 3. Cont.

| Ref. | Topology | Advantages | Disadvantages | Inverter Size | Maximum Efficiency | No. Conversion Stages | Leakage Current | Control Strategy |
|------|-------------|---|-----------------------|---------------|--------------------|-----------------------|-----------------|------------------|
| [53] | Standard H6 | Low output current ripple and I_{cm} . Constant CM voltage. | Diode conduction loss | Medium | 97.5% | 1 | Low | Medium |

Finally, the efficiency of the different topologies is compared in Figure 13 for both inversion and rectifier modes. These results have been extracted from the measurement data presented in the publications. For a fair comparison, ref [63] was excluded since its power is significantly lower (300 W). As can be seen, the majority of topologies provide relatively high efficiency at full load. It is worth noting that the highest efficiency of [43] comes from using 75 A oversized semiconductor devices at 3 kW. The next highest efficiency is achieved with a two-stage solution that includes CM decoupling, but it has high cost and size due to additional components. Next comes the H6 topology [48], but its efficiency drops rapidly at low power.

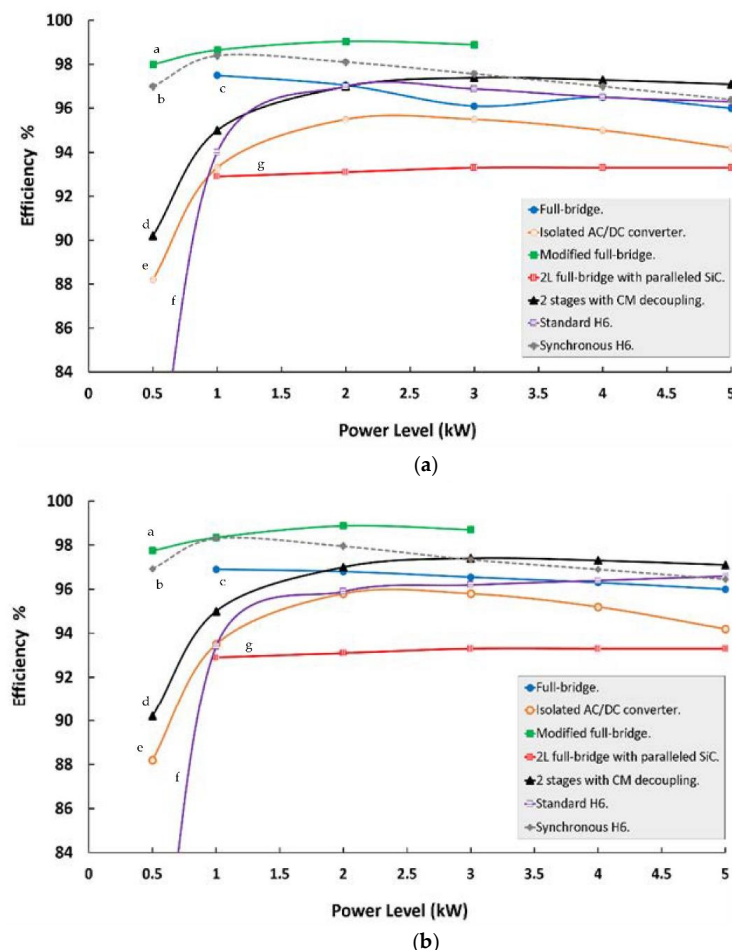


Figure 13. Bidirectional inverter efficiency comparison curves of (a) inversion mode, (b) rectification mode. a—[43]; b—[54]; c—[52]; d—[57]; e—[51]; f—[53]; g—[56].

However, a residential building will generally operate at a lower load than its maximum rated over the majority of the time. Therefore, bidirectional inverters with low efficiency at light loads would impact the overall system efficiency. The evaluation of the

synchronous H6 using PSIM software with detailed analytic equations applied to predict component power loss for suitably sized semiconductors shows that the light load efficiency of the standard H6 can be addressed by replacing diodes with MOSFETs, as explained in [54].

5. Smart Grid Control

The control system is an important component of grid-connected power converters where it maintains the system efficiency and stability. Integrating a DC system into the grid may cause several issues, including grid instability and disruption, so several control solutions have been proposed to overcome grid distortions and fulfill the criteria of the grid's standard power [80,81].

The main control system requirement is as follows: phase estimation, which is known as a phase-locked loop (PLL), voltage control loop (VCL), and current control loop (CCL), as shown in Figure 14. The PLL is used to generate the grid reference current, which is synchronous with the grid voltage, where the most implemented type is the basic PLL in such applications. The DC-bus voltage is regulated by the use of a VCL that produces the required grid current amplitude to be compared with the grid current reference obtained from the PLL. The inductor current needs to be compared with the grid current to determine the duty cycle and track any sudden change through a CCL. The performance of the control system can best be treated according to the following tasks:

- Reactive power control for supplying the DC system.
- Active power control for feeding the grid.
- DC-bus voltage control.
- Grid synchronization.
- Dynamic operational modes control (inverter/rectifier).

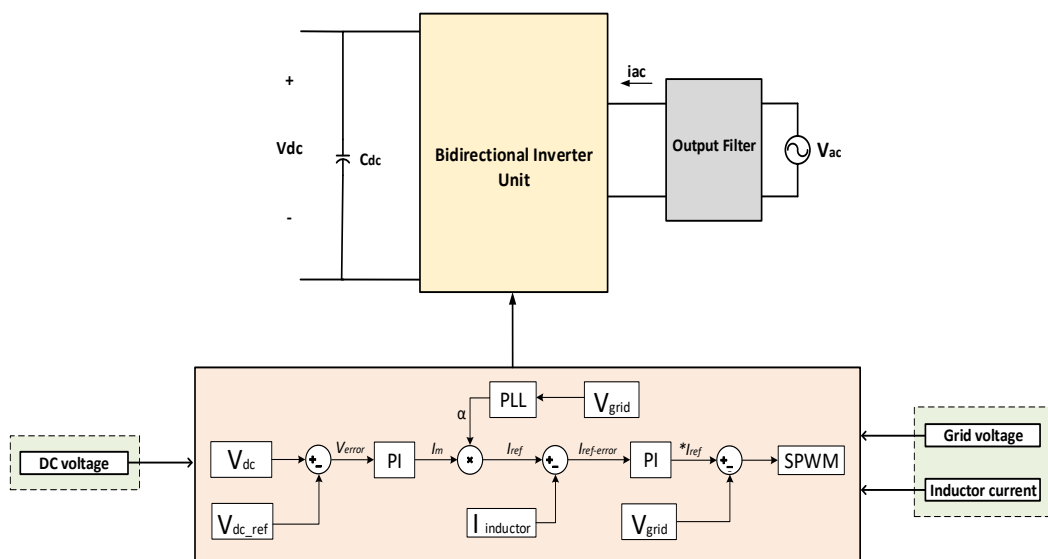


Figure 14. General configuration of the bidirectional inverter control system.

There is a possible classification of bidirectional inverter control systems based on a comparison of the following criteria: DC-bus voltage regulation, inductor current control, and bidirectional capability. This section provides a basis for comparison to enable the identification of the control system structure and to distinguish different levels of performance.

5.1. Controller Challenges

5.1.1. DC-Bus Voltage Regulation

The integration of a DC bus with different types of energy sources such as renewable energy and energy storage may result in system instability; therefore, the bus voltage needs

to be retained at a nominal level to enable the reliable operation of the grid, battery, and DC loads. Regulating a DC bus is challenging due to the wide range of load and source conditions that it is expected to support, and the introduction of current harmonics through the grid connection. This issue was examined in [45], where fast regulation control is suggested to track any sudden change of bus voltage every quarter cycle. Likewise, the authors of [47,49] propose a quarter cycle approach (QLCRA) to regulate the variation in DC-bus voltage in situations where the integrated grid interface causes AC current distortion. The distorted line current was minimized when the inductor current was adjusted each quarter cycle instead of the conventional line cycle approach (OLCRA). The bus voltage also can vary when there are more input sources connected to the system.

The study of [42] applied predictive control to track an AC current reference by sensing the inductor current to obtain the desired output bus voltage. The stability of the bus voltage is achieved during both inversion and rectification modes. There is, however, a noticeable current distortion during the phase shift transition between these two modes, particularly at zero crossing, due to insufficient magnetizing inductor current. To achieve high power quality, two switching schemes were compared: unipolar and bipolar for delivering and consuming the utility grid power, respectively [46]. It was found that insufficient inductor current causes current distortion in unipolar operation, whereas bipolar operation decreases the distortion but induces higher current ripple and switching loss. The combined PWM schemes reduced the current distortion and at the same time relatively decreased the voltage ripple and switching loss. As a result, the unipolar system is deemed to be better in terms of lower voltage ripple and switching loss in both inversion and rectification modes.

However, a particular frequency response for designing the AC filter is required to eliminate the applied high frequency on switches, besides the switching loss when using a bipolar scheme. Alternatively, half of the switches in the bridge may be operated at high frequency, while low frequency is applied to the other switches with a hysteresis switching scheme [82]. It is worth mentioning that the switching loss for the hysteresis scheme has the same loss as the unipolar scheme [83].

Moreover, to ensure consistent frequency operation during zero-crossing, it is necessary to consider the DC-link voltage ripple and inductor current harmonics. In fact, high-frequency operation could result in a significant distortion of the delivered grid voltage caused by the dead time control aspect. As a result, the authors of [84] proposed a single switch to operate during the transient period when mode switching occurs in which a freewheeling path is provided to sustain the inductor current. This technique relies on the idea of miniaturizing the leakage current, which is still not optimal. Since the employed semiconductor devices were designed on the maximum operating current level, there is an additional potential cost-related consideration.

5.1.2. Inductor Nonlinearity

Recent developments in bidirectional inverters have heightened the need for controlling the nonlinearity of the inductor current that might occur in one operational cycle due to the inductance variation of different core materials over a wide range of currents. Consequently, a high current ripple has an impact on the accuracy of tracking the inductor current to generate the required duty ratio. Therefore, the authors of [52,77] proposed a predictive control technique to mitigate this variation by sensing the inductor current and using the grid and DC-bus voltage as iteration variables for determining the required duty ratio for the next cycle. However, it is expected that the proposed control is almost certainly limited when the system is subjected to a high load profile resulting in a voltage drop. In contrast to the earlier study, however, no evidence of reducing the current distortion was reported. According to [50,85] a fuzzy logic controller strategy is recommended to overcome the mentioned issue by increasing the inductor voltage to enable the fast-tracking of the current reference. It is believed that the fluctuation of the inductance current peak waveform was minimized; however, there is still some spiking in the zero-crossing point due to the line frequency operation. The strategies of applying low-frequency control to improve the

inductor current oscillation might involve current sharing between the switches' parasitic capacitor which leads to a decrease in efficiency. Therefore, high-frequency operation can reduce the shared current in certain topology configurations that utilize middle switches (floating switches). In addition, the controller's bandwidth can be increased to enhance load transient response.

Despite this, little progress has been made with regard to deploying a high-resolution current for sensing the AC-side current during a rapid change of the inductor current. Analog-to-Digital converters (ADCs) can be adapted to achieve the required accuracy response under a wide range of the grid current. However, the implementation of ADCs suffers from higher complexity and higher cost. As a result, it has been shown conclusively that the continuous conducting mode (CCM) of the inductor current (rather than discontinuous conducting mode (DCM)) is desirable due to the simplicity of implementation in which the current measurement was replaced by a practical sensorless, average current regulation control algorithm model [86,87]. Nevertheless, it is important that other factors can affect the sensing procedure of the inner current loop control, such as inductance, inductor resistance, and related voltage conduction [88,89]. Therefore, the authors of [40] developed a sensorless current control with bidirectional capability to enhance the functionality of the PFC during the grid injection. It seems possible that a transient current is expected to contribute to the associated dynamic decoupling between DC and AC sides, in which a significant response time is required during a change of mode. Collectively, these studies outline a critical role for inductance variation on the system performance, which potentially needs to be taken into consideration.

5.1.3. Bidirectional Capability

The correlation of the inductor current and the DC-bus voltage has an influence on the transition region between inversion and rectification, as depicted in Figure 15. As can be seen, a linear relationship between the inductor current and DC-bus voltage determines the operation mode of the power flow. It is important to note that the DC-bus voltage should be operated in a range of $\pm 10\%$ Vdc in order to avoid frequent changes of mode during a sudden heavy load. As a result, it is possible that current distortion occurs during the transition period in the zero-crossing voltage. There is some evidence to suggest that PFC compensation could be utilized when the magnetization current is inadequate to mitigate the phase-shift region [46]. However, the time required to adjust the duty cycle for changing the switching mode is considered relatively slow, where a fast control response is needed in such conditions. This indicates a need to understand the various aspects of control ability that exist in two-stage power conversion topology, especially in the isolated DC/DC stage. This may lead to an inappropriate escalation in uncontrolled power conversion mode when the load demand becomes negative, resulting in a significant increase in the delivered power to the output capacitor due to the combination of load and converter terminal.

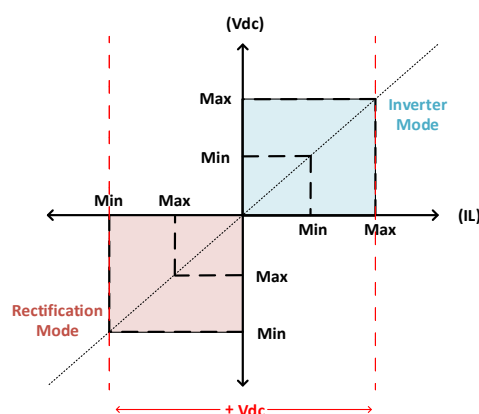


Figure 15. The regulation technique of DC-bus voltage (V_{dc}) with associated linearity of relationship with the inductor current (I_L).

The authors of [51] set out a proposal of employing a dead-band control algorithm to smooth any abrupt state in performance where the DC-bus voltage is varying in two-stage systems. However, the utilized controller is not autonomous because an additional slave controller is required for the integrated power conversion stages. In contrast, the authors of [90] offer a fly-back bidirectional control capability using a single power conversion stage to overcome the complex implementation of controllers required in isolated two-stage converters. This is suitable only for integration between the energy storage and utility grid, which can be adapted for integration with DC distribution systems. Perhaps the most serious disadvantage of this technique is that a significant voltage and current stress is imposed on the converter semiconductors, which has been thought of as a key factor in system efficiency and performance. The distinctions between single-stage and two-stage bidirectional power conversion, with respect to which isolation's value is evaluated, are evidently a significant constraint on all the work discussed in this area.

A comparison summary of the implemented control is presented in Table 4.

Table 4. Summary of control implementation of transformer and transformerless bidirectional topologies for DC distribution systems.

| Ref. | Advantages | Disadvantages | Controller Type |
|---------|---|--|-----------------|
| [51,55] | Fast dynamic response Low THD | Complex control structure | Hysteresis |
| [52,77] | Fast dynamic response Easy implementation | More calculation required | Predictive |
| [45] | Reactive power control High dynamic | Complex control structure High THD | Predictive |
| [46] | Simplicity | No full PFC Two controllers | - |
| [47,49] | Instantaneous current control Less circuitry | Complex transfer function | Predictive |
| [42] | High dynamic Low THD | Complex transfer function | Fuzzy logic |
| [50] | Lower inductor current ripple | High THD No full control of PFC | Fuzzy logic |
| [40] | One inductor filter | Slow tracking response No full control of PFC | Predictive |
| [58] | Fast tracking and dynamic response High gain | Limited operational range | Resonant |

6. Conclusions

In this review, the aim is to assess the performance of existing bidirectional inverter topologies integrated with a DC distribution system in which renewable energy sources, energy storage, and DC loads are used. It was found that transformerless topologies outweigh transformer-based topologies due to higher efficiency and smaller size of the power converters. However, the primary issue with transformerless topologies is the connection between the utility grid and the DC bus, which results in high leakage current and high CMV, which have a negative effect on the overall efficiency. Freewheeling paths and two-stage power conversion are the prominent solutions for the drawbacks of transformerless topologies. It was found that the standard H6 topology provides the best performance in terms of high efficiency and cost-benefit related to the semiconductor devices and passive components required to eliminate leakage current and CMV. However, it is important to note that the efficiency of this topology decreases significantly when operating at less than 20% of its maximum rated power (5 kW) compared to other transformerless topologies.

The present study adds to the growing body of research regarding DC distribution systems that aim to enhance the system efficiency of power delivery between DC power sources, loads, and energy storage devices over AC distribution. It was shown that there is scope for further research on methods to improve the efficiency of bidirectional topologies under light-load conditions, and the dynamic response of control systems in two-stage bidirectional power converters. Furthermore, while the requirements of bidirectional inverters integrated with DC distribution in buildings may not be compatible for use in different applications such as (EV) and energy storage, the circuit topologies and control methods described may be adapted for other bidirectional applications. In conclusion, it is believed that this review will provide a reference for academics, engineers, manufacturers, and end-users interested in implementing DC distribution systems using bidirectional inverters with grid-connected and renewable energy systems.

Author Contributions: Conceptualization, M.A. and M.D.; methodology, M.A. and M.D.; software, M.A.; validation, M.A. and M.D.; formal analysis M.A.; investigation, M.A.; resources, M.A. and M.D.; data curation, M.A.; writing—original draft preparation, M.A.; writing—review and editing, M.D.; visualization, M.A. and M.D.; supervision, M.D.; project administration, M.A. and M.D.; funding acquisition, M.D. All authors have read and agreed to the published version of the manuscript.

Funding: This review paper was invited by the editor of Energies to the corresponding author.

Institutional Review Board Statement: Not applicable.

Informed Consent Statement: Not applicable.

Data Availability Statement: Not applicable.

Conflicts of Interest: The authors declare no conflict of interest.

References

1. Kannan, N.; Vakeesan, D. Solar energy for future world: A review. *Renew. Sustain. Energy Rev.* **2016**, *62*, 1092–1105. [[CrossRef](#)]
2. Garbesi, K.; Vossos, V.; Shen, H. *Catalog of DC Appliances and Power Systems*; Lawrence Berkeley National Laboratory: Berkeley, CA, USA, 2012; pp. 1–77. [[CrossRef](#)]
3. EMerge Alliance.pdf. Available online: <https://www.emergealliance.org/standards/our-standards/> (accessed on 1 October 2021).
4. Sabry, A.H.; Shallal, A.H.; Hameed, H.S.; Ker, P.J. Compatibility of household appliances with DC microgrid for PV systems. *Heliyon* **2020**, *6*, e05699. [[CrossRef](#)] [[PubMed](#)]
5. U.S. Energy Information Administration. Available online: <https://www.eia.gov/> (accessed on 1 October 2021).
6. Glasgo, B.; Azevedo, I.L.; Hendrickson, C. How much electricity can we save by using direct current circuits in homes? Understanding the potential for electricity savings and assessing feasibility of a transition towards DC powered buildings. *Appl. Energy* **2016**, *180*, 66–75. [[CrossRef](#)]
7. Vossos, V.; Garbesi, K.; Shen, H. Energy savings from direct-DC in U.S. residential buildings. *Energy Build.* **2014**, *68*, 223–231. [[CrossRef](#)]
8. Kakigano, H.; Nomura, M.; Ise, T. Loss evaluation of DC distribution for residential houses compared with AC system. In Proceedings of the 2010 International Power Electronics Conference-ECCE Asia, Sapporo, Japan, 21–24 June 2010; pp. 480–486. [[CrossRef](#)]
9. Liu, Z.; Li, M. Research on Energy Efficiency of DC Distribution System. *AASRI Procedia* **2014**, *7*, 68–74. [[CrossRef](#)]
10. Alshammari, M.; Duffy, M. Feasibility Analysis of a DC Distribution System for a 6 kW Photovoltaic Installation in Ireland. *Energies* **2021**, *14*, 6265. [[CrossRef](#)]
11. Chauhan, R.K.; Rajpurohit, B.S. DC distribution system for energy efficient buildings. In Proceedings of the 2014 Eighteenth National Power Systems Conference (NPSC), Guwahati, India, 18–20 December 2014; pp. 1–6. [[CrossRef](#)]
12. Palaniappan, K.; Veerapeneni, S.; Cuzner, R.; Zhao, Y. Assessment of the feasibility of interconnected smart DC homes in a DC microgrid to reduce utility costs of low income households. In Proceedings of the 2017 IEEE Second International Conference on DC Microgrids (ICDCM), Nuremberg, Germany, 27–29 June 2017; pp. 467–473. [[CrossRef](#)]
13. Boeke, U.; Wendt, M. DC power grids for buildings. In Proceedings of the 2015 IEEE First International Conference on DC Microgrids (ICDCM), Atlanta, GA, USA, 7–10 June 2015; pp. 210–214. [[CrossRef](#)]
14. Alshammari, M.; Duffy, M. Comparative analysis between AC and DC distribution systems in a photovoltaic system: A case study of a school in Ireland. In Proceedings of the PCIM Europe 2019; International Exhibition and Conference for Power Electronics, Intelligent Motion, Renewable Energy and Energy Management, Nuremberg, Germany, 7–9 May 2019; pp. 1–8.

15. Estévez-Bén, A.A.; Alvarez-Diazcomas, A.; Macias-Bobadilla, G.; Rodríguez-Reséndiz, J. Leakage Current Reduction in Single-Phase Grid-Connected Inverters—A Review. *Appl. Sci.* **2020**, *10*, 2384. [[CrossRef](#)]
16. Guo, X.; Jia, X. Hardware-Based Cascaded Topology and Modulation Strategy with Leakage Current Reduction for Transformerless PV Systems. *IEEE Trans. Ind. Electron.* **2016**, *63*, 7823–7832. [[CrossRef](#)]
17. Wu, T.-F.; Kuo, C.-L.; Sun, K.-H.; Chen, Y.-K.; Chang, Y.-R.; Lee, Y.-D. Integration and Operation of a Single-Phase Bidirectional Inverter with Two Buck/Boost MPPTs for DC-Distribution Applications. *IEEE Trans. Power Electron.* **2013**, *28*, 5098–5106. [[CrossRef](#)]
18. Ryu, M.-H.; Kim, H.-S.; Baek, J.-W.; Kim, H.-G.; Jung, J.-H. Effective Test Bed of 380-V DC Distribution System Using Isolated Power Converters. *IEEE Trans. Ind. Electron.* **2015**, *62*, 4525–4536. [[CrossRef](#)]
19. Yang, Y.; Wang, H.; Blaabjerg, F. Reactive power injection strategies for single-phase photovoltaic systems considering grid requirements. *IEEE Trans. Ind. Appl.* **2014**, *50*, 4065–4076. [[CrossRef](#)]
20. Robles, O.E.O.; Beristain, J.A.; Ramírez, J.P. Single-phase bidirectional high frequency link photovoltaic inverter with reactive power compensation function. In Proceedings of the 2015 IEEE Workshop on Power Electronics and Power Quality Applications (PEPQA), Bogota, Colombia, 2–4 June 2015; pp. 1–6. [[CrossRef](#)]
21. Vancu, M.F.; Soeiro, T.; Muhlethaler, J.; Kolar, J.W.; Aggeler, D. Comparative evaluation of bidirectional buck-type PFC converter systems for interfacing residential DC distribution systems to the smart grid. In Proceedings of the 2012 IECON Proceedings (Industrial Electronics Conference), Montreal, QC, Canada, 25–28 October 2012; pp. 5153–5160. [[CrossRef](#)]
22. Dong, D. Ac-dc Bus-interface Bi-Directional Converters in Renewable Energy Systems. Ph.D. Thesis, Virginia Polytechnic Institute and State University, Ann Arbor, MN, USA, 2012.
23. Dong, D.; Cvetkovic, I.; Boroyevich, D.; Zhang, W.; Wang, R.; Mattavelli, P. Grid-Interface Bidirectional Converter for Residential DC Distribution Systems—Part One: High-Density Two-Stage Topology. *IEEE Trans. Power Electron.* **2012**, *28*, 1655–1666. [[CrossRef](#)]
24. Rawat, G.S. Sathans Survey on DC microgrid architecture, power quality issues and control strategies. In Proceedings of the 2nd International Conference on Inventive Systems and Control (ICISC), Coimbatore, India, 19–20 January 2018; pp. 500–505. [[CrossRef](#)]
25. Rodriguez-Diaz, E.; Savaghebi, M.; Vasquez, J.C.; Guerrero, J.M. An overview of low voltage DC distribution systems for residential applications. In Proceedings of the 2015 IEEE 5th International Conference on Consumer Electronics—Berlin (ICCE-Berlin), Berlin, Germany, 6–9 September 2015. [[CrossRef](#)]
26. Ghareeb, A.T.; Mohamed, A.A.; Mohammed, O.A. DC microgrids and distribution systems: An overview. In Proceedings of the IEEE Power and Energy Society General Meeting, Vancouver, BC, Canada, 21–25 July 2013.
27. Liu, P.; Wu, Z.; Gu, W.; Lu, Y.; Yang, X.; Sun, K.; Sun, Q. Security-constrained AC–DC hybrid distribution system expansion planning with high penetration of renewable energy. *Int. J. Electr. Power Energy Syst.* **2022**, *142*, 108285. [[CrossRef](#)]
28. Subudhi, B.; Pradhan, R. A Comparative Study on Maximum Power Point Tracking Techniques for Photovoltaic Power Systems. *IEEE Trans. Sustain. Energy* **2012**, *4*, 89–98. [[CrossRef](#)]
29. Chauhan, R.K.; Rajpurohit, B.S.; Hebner, R.E.; Singh, S.N.; Gonzalez-Longatt, F.M. Voltage Standardization of DC Distribution System for Residential Buildings. *J. Clean Energy Technol.* **2015**, *4*, 167–172. [[CrossRef](#)]
30. Dragičević, T.; Guerrero, J.M. DC Microgrids—Part II: A Review of Power Architectures, Applications, and Standardization Issues. *IEEE Trans. Power Electron.* **2016**, *31*, 3528–3549.
31. Dragičević, T.; Lu, X.; Vasquez, J.C.; Guerrero, J.M. DC Microgrids—Part I: A Review of Control Strategies and Stabilization Techniques. *IEEE Trans. Power Electron.* **2016**, *31*, 4876–4891. [[CrossRef](#)]
32. Jung, T.-H.; Gwon, G.-H.; Kim, C.-H.; Han, J.; Oh, Y.-S.; Noh, C.-H. Voltage Regulation Method for Voltage Drop Compensation and Unbalance Reduction in Bipolar Low-Voltage DC Distribution System. *IEEE Trans. Power Deliv.* **2017**, *33*, 141–149. [[CrossRef](#)]
33. Wu, T.-F.; Chang, C.-H.; Lin, L.-C.; Yu, G.-R.; Chang, Y.-R. DC-Bus Voltage Control with a Three-Phase Bidirectional Inverter for DC Distribution Systems. *IEEE Trans. Power Electron.* **2012**, *28*, 1890–1899. [[CrossRef](#)]
34. Riccobono, A.; Santi, E. Comprehensive Review of Stability Criteria for DC Power Distribution Systems. *IEEE Trans. Ind. Appl.* **2014**, *50*, 3525–3535. [[CrossRef](#)]
35. Kakigano, H.; Miura, Y.; Ise, T. Low-Voltage Bipolar-Type DC Microgrid for Super High Quality Distribution. *IEEE Trans. Power Electron.* **2010**, *25*, 3066–3075. [[CrossRef](#)]
36. Mishra, A.; Rajeev, K.; Garg, V. Assessment of 48 volts DC for homes. In Proceedings of the 2018 IEEMA Engineer Infinite Conference (eTechNxT 2018), New Delhi, India, 13–14 March 2018; pp. 1–6. [[CrossRef](#)]
37. Dastgeer, F.; Gelani, H.E. A Comparative analysis of system efficiency for AC and DC residential power distribution paradigms. *Energy Build.* **2017**, *138*, 648–654. [[CrossRef](#)]
38. Chen, F.; Burgos, R.; Boroyevich, D. A high-efficiency interleaved single-phase AC–DC converter with common-mode voltage regulation for 380 VDC microgrids. In Proceedings of the 2017 IEEE Energy Conversion Congress and Exposition (ECCE), Cincinnati, OH, USA, 1–5 October 2017; pp. 4128–4135.
39. Hwang, J.-C.; Chen, P.-C.; Liu, C.-S.; Chen, L.-R. A novel single-phase interleaved Bi-directional inverter for grid-connection control. *IEEE Int. Symp. Ind. Electron.* **2014**, *43*, 375–379. [[CrossRef](#)]
40. Chen, H.-C.; Liao, J.-Y. Bidirectional Current Sensorless Control for the Full-Bridge AC/DC Converter with Considering Both Inductor Resistance and Conduction Voltages. *IEEE Trans. Power Electron.* **2013**, *29*, 2071–2082. [[CrossRef](#)]

41. Sathler, H.H.; Marcelino, F.L.F.; de Oliveira, T.R.; Seleme, S.I.; Garcia, P.F.D. A comparative efficiency study on bidirectional grid interface converters applied to low power DC nanogrids. In Proceedings of the 14th Brazilian Power Electronics Conference COBEP 2017, Juiz de Fora, Brazil, 19–22 November 2017; pp. 1–6. [CrossRef]
42. Yu, G.-R.; Wei, J.-S. Modeling and control of a bi-directional inverter for DC microgrids. In Proceedings of the 2011 International Conference on System Science and Engineering (ICSSE), Macau, China, 8–10 June 2011; pp. 425–430. [CrossRef]
43. Lee, S.; Kim, K.; Kwon, J.; Kwon, B. Single-phase transformerless bi-directional inverter with high efficiency and low leakage current. *IET Power Electron.* **2014**, *7*, 451–458. [CrossRef]
44. Dong, D.; Luo, F.; Boroyevich, D.; Mattavelli, P. Leakage Current Reduction in a Single-Phase Bidirectional AC–DC Full-Bridge Inverter. *IEEE Trans. Power Electron.* **2012**, *27*, 4281–4291. [CrossRef]
45. Wu, T.-F.; Kuo, C.-L.; Sun, K.-H.; Chang, Y.-C. Dc-bus voltage regulation and power compensation with bi-directional inverter in dc-microgrid applications. In Proceedings of the 2011 IEEE Energy Conversion Congress and Exposition, Phoenix, AZ, USA, 17–22 September 2011; pp. 4161–4168. [CrossRef]
46. Wu, T.-F.; Kuo, C.-L.; Sun, K.-H.; Chang, Y.-C. Current distortion improvement for power compensation with bi-directional inverter in DC-distribution system. In Proceedings of the 2012 15th International Power Electronics and Motion Control Conference (EPE/PEMC), Novi Sad, Serbia, 4–6 September 2012; pp. 1–7. [CrossRef]
47. Wu, T.-F.; Kuo, C.-L.; Sun, K.-H.; Yu, G.-R. DC-bus voltage regulation with bi-directional inverter in DC distribution systems. In Proceedings of the IEEE Applied Power Electronics Conference and Exposition (APEC), Orlando, FL, USA, 5–9 February 2012; pp. 769–774. [CrossRef]
48. Chen, Y.-K.; Wu, T.-F.; Chang, Y.-C.; Lin, L.-C.; Yao, N. Extended Application of D-\$\{\backslash bf \Sigma\}\$ Digital Control to a Single-Phase Bidirectional Inverter With an LCL Filter. *IEEE Trans. Power Electron.* **2014**, *30*, 3903–3911.
49. Wu, T.-F.; Kuo, C.-L.; Lin, L.-C.; Chen, Y.-K. DC-Bus Voltage Regulation for a DC Distribution System with a Single-Phase Bidirectional Inverter. *IEEE J. Emerg. Sel. Top. Power Electron.* **2015**, *4*, 210–220. [CrossRef]
50. Yu, G.-R.; Lai, J.-J.; Liu, J.-Y. T-S fuzzy control of a single-phase bidirectional inverter. *Proc. IEEE Int. Conf. Ind. Technol.* **2016**, *2016*, 1462–1467. [CrossRef]
51. Kim, H.-S.; Ryu, M.-H.; Baek, J.-W.; Jung, J.-H. High-Efficiency Isolated Bidirectional AC–DC Converter for a DC Distribution System. *IEEE Trans. Power Electron.* **2012**, *28*, 1642–1654. [CrossRef]
52. Wu, T.-F.; Sun, K.-H.; Kuo, C.-L.; Chang, C.-H. Predictive Current Controlled 5-kW Single-Phase Bidirectional Inverter With Wide Inductance Variation for DC-Microgrid Applications. *IEEE Trans. Power Electron.* **2010**, *25*, 3076–3084. [CrossRef]
53. Wang, J.; Gao, S.; Sun, Y.; Ji, Z.; Cheng, L.; Li, L.; Gu, W.; Zhao, J. Single Phase Bidirectional H6 Rectifier/Inverter. *IEEE Trans. Power Electron.* **2019**, *34*, 10710–10719. [CrossRef]
54. Alshammari, M.; Duffy, M. A novel synchronous H6 for improving light load efficiency of bidirectional inverters in a DC distribution system. In Proceedings of the 2021 IEEE Applied Power Electronics Conference and Exposition (APEC), Phoenix, AZ, USA, 14–17 June 2021; pp. 1666–1673. [CrossRef]
55. Jung, J.-H.; Kim, H.-S.; Ryu, M.-H.; Kim, J.-H.; Baek, J.-W. Single-phase bidirectional AC–DC boost rectifier for DC distribution system. In Proceedings of the 2013 IEEE ECCE Asia Downunder-5th IEEE Annual International Energy Conversion Congress and Exhibition, IEEE ECCE Asia 2013, Melbourne, Australia, 3–6 June 2013; pp. 544–549. [CrossRef]
56. Chen, F.; Burgos, R.; Boroyevich, D. Efficiency comparison of a single-phase grid-interface bidirectional AC/DC converter for DC distribution systems. In Proceedings of the 2015 IEEE Energy Conversion Congress and Exposition (ECCE), Montreal, QC, Canada, 20–24 September 2015; pp. 6261–6268. [CrossRef]
57. Chen, F.; Burgos, R.; Boroyevich, D. A Bidirectional High-Efficiency Transformerless Converter with Common-Mode Decoupling for the Interconnection of AC and DC Grids. *IEEE Trans. Power Electron.* **2018**, *34*, 1317–1333. [CrossRef]
58. Chen, F.; Burgos, R.; Boroyevich, D.; Dong, D. Control loop design of a two-stage bidirectional AC/DC converter for renewable energy systems. In Proceedings of the 2014 IEEE Applied Power Electronics Conference and Exposition-APEC 2014, Fort Worth, TX, USA, 16–20 March 2014; pp. 2177–2183. [CrossRef]
59. Du, W.; Jiang, Q.; Erickson, M.J.; Lasseter, R.H. Voltage-Source Control of PV Inverter in a CERTS Microgrid. *IEEE Trans. Power Deliv.* **2014**, *29*, 1726–1734. [CrossRef]
60. Wiechmann, E.P.; Aqueveque, P.; Burgos, R.; Rodriguez, J. On the Efficiency of Voltage Source and Current Source Inverters for High-Power Drives. *IEEE Trans. Ind. Electron.* **2008**, *55*, 1771–1782. [CrossRef]
61. Singh, J.; Dahiya, R.; Saini, L.M. Recent research on transformer based single DC source multilevel inverter: A review. *Renew. Sustain. Energy Rev.* **2018**, *82*, 3207–3224. [CrossRef]
62. Khan, N.H.; Forouzesh, M.; Siwakoti, Y.P.; Li, L.; Kerekes, T.; Blaabjerg, F. Transformerless Inverter Topologies for Single-Phase Photovoltaic Systems: A Comparative Review. *IEEE J. Emerg. Sel. Top. Power Electron.* **2019**, *8*, 805–835. [CrossRef]
63. Wu, T.-F.; Wang, S.-A.; Kuo, C.-L.; Lee, K.-Y. Design and implementation of a push-pull phase-shifted bi-directional inverter with a dsPIC controller. In Proceedings of the International Conference on Power Electronics and Drive Systems (PEDS 2009), Taipei, Taiwan, 2–5 January 2009; pp. 728–733. [CrossRef]
64. Ortiz, G.; Biela, J.; Bortis, D.; Kolar, J.W. Converter for Renewable Energy Applications Converter for Renewable Energy Applications. In Proceedings of the 2010 International Power Electronics Conference-ECCE ASIA, Sapporo, Japan, 21–24 June 2010; pp. 3212–3219.

65. Sabry, A.H.; Mohammed, Z.M.; Nordin, F.H.; Ali, N.H.N.; Al-Ogaili, A.S. Single-Phase Grid-Tied Transformerless Inverter of Zero Leakage Current for PV System. *IEEE Access* **2019**, *8*, 4361–4371. [[CrossRef](#)]
66. Ge, W.; Wang, Y.; Zhao, Z.; Yang, X.; Li, Y. Residual Flux in the Closed Magnetic Core of a Power Transformer. *IEEE Trans. Appl. Supercond.* **2013**, *24*, 1–4. [[CrossRef](#)]
67. Otero-De-Leon, R.; Mohan, N. A push-pull DC-AC high frequency power electronics transformer for photovoltaic applications. In Proceedings of the IECON Proceedings (Industrial Electronics Conference) 2014, Dallas, TX, USA, 29 October–1 November 2014; pp. 1131–1136. [[CrossRef](#)]
68. Pan, X.; Li, H.; Liu, Y.; Zhao, T.; Ju, C.; Gae, A.K.R. An Overview and Comprehensive Comparative Evaluation of Current-Fed-Isolated-Bidirectional DC/DC Converter. *IEEE Trans. Power Electron.* **2019**, *35*, 2737–2763. [[CrossRef](#)]
69. Xue, F.; Yu, R.; Huang, A.Q. A 98.3% Efficient GaN Isolated Bidirectional DC-DC Converter for DC Microgrid Energy Storage System Applications. *IEEE Trans. Ind. Electron.* **2017**, *64*, 9094–9103. [[CrossRef](#)]
70. Wu, T.-F.; Chen, Y.-C.; Yang, J.-G.; Kuo, C.-L. Isolated Bidirectional Full-Bridge DC-DC Converter With a Flyback Snubber. *IEEE Trans. Power Electron.* **2010**, *25*, 1915–1922. [[CrossRef](#)]
71. Naayagi, R.T.; Forsyth, A.J.; Shuttleworth, R. High-Power Bidirectional DC-DC Converter for Aerospace Applications. *IEEE Trans. Power Electron.* **2012**, *27*, 4366–4379. [[CrossRef](#)]
72. Chen, W.; Rong, P.; Lu, Z. Snubberless Bidirectional DC-DC Converter With New CLLC Resonant Tank Featuring Minimized Switching Loss. *IEEE Trans. Ind. Electron.* **2009**, *57*, 3075–3086. [[CrossRef](#)]
73. López, O.; Freijedo, F.D.; Yépes, A.G.; Fernández-Comesaña, P.; Malvar, J.; Teodorescu, R. Eliminating ground current in a transformerless photovoltaic application. *IEEE Trans. Energy Convers.* **2010**, *25*, 140–147. [[CrossRef](#)]
74. Ji, B.; Wang, J.; Zhao, J. High-Efficiency Single-Phase Transformerless PV H6 Inverter With Hybrid Modulation Method. *IEEE Trans. Ind. Electron.* **2012**, *60*, 2104–2115. [[CrossRef](#)]
75. Wang, J.; Luo, F.; Ji, Z.; Sun, Y.; Ji, B.; Gu, W.; Zhao, J. An Improved Hybrid Modulation Method for the Single-Phase H6 Inverter with Reactive Power Compensation. *IEEE Trans. Power Electron.* **2017**, *33*, 7674–7683. [[CrossRef](#)]
76. Chen, F.; Burgos, R.; Boroyevich, D.; Zhang, X. Low-Frequency Common-Mode Voltage Control for Systems Interconnected with Power Converters. *IEEE Trans. Ind. Electron.* **2016**, *64*, 873–882. [[CrossRef](#)]
77. Wu, T.-F.; Sun, K.-H.; Kuo, C.-L.; Yang, M.-S.; Chang, R.-C. Design and implementation of a 5 kW 1φ bi-directional inverter with wide inductance variation. In Proceedings of the 2010 IEEE Energy Conversion Congress and Exposition, Atlanta, GA, USA, 12–16 September 2010; pp. 45–52. [[CrossRef](#)]
78. Yu, G.-R.; Wei, J.-S. Fuzzy control of a bi-directional inverter with nonlinear inductance for DC microgrids. In Proceedings of the 2011 IEEE International Conference on Fuzzy Systems, Taipei, Taiwan, 27–30 June 2011; pp. 1941–1945. [[CrossRef](#)]
79. Liu, C.; Wang, Y.; Cui, J.; Zhi, Y.; Liu, M.; Cai, G. Transformerless Photovoltaic Inverter Based on Interleaving High-Frequency Legs Having Bidirectional Capability. *IEEE Trans. Power Electron.* **2016**, *31*, 1131–1142. [[CrossRef](#)]
80. Nejabatkhah, F.; Li, Y.W.; Tian, H. Power Quality Control of Smart Hybrid AC/DC Microgrids: An Overview. *IEEE Access* **2019**, *7*, 52295–52318. [[CrossRef](#)]
81. Nejabatkhah, F.; Li, Y.W. Overview of Power Management Strategies of Hybrid AC/DC Microgrid. *IEEE Trans. Power Electron.* **2014**, *30*, 7072–7089. [[CrossRef](#)]
82. Li, R.T.H.; Chung, H.S.-H.; Lau, W.-H.; Zhou, B. Use of Hybrid PWM and Passive Resonant Snubber for a Grid-Connected CSI. *IEEE Trans. Power Electron.* **2010**, *25*, 298–309. [[CrossRef](#)]
83. Lai, R.; Ngo, K.D.T. A PWM method for reduction of switching loss in a full-bridge inverter. *IEEE Trans. Power Electron.* **1995**, *10*, 326–332.
84. Liao, Y.-H. A Novel Reduced Switching Loss Bidirectional AC/DC Converter PWM Strategy with Feedforward Control for Grid-Tied Microgrid Systems. *IEEE Trans. Power Electron.* **2013**, *29*, 1500–1513. [[CrossRef](#)]
85. Zheng, Z.; Zhang, T.; Xue, J. Application of Fuzzy Control in a Photovoltaic Grid-Connected Inverter. *J. Electr. Comput. Eng.* **2018**, *2018*, 3806372. [[CrossRef](#)]
86. Suzdalenko, A. Current Sensorless Control of Front-end Bidirectional AC/DC Converter Based on Half-bridge Topology. *Electr. Control Commun. Eng.* **2013**, *4*, 19–25. [[CrossRef](#)]
87. Suzdalenko, A. Development of single-switch model for current sensorless control of bidirectional half-bridge AC/DC converter. In Proceedings of the 2014 55th International Scientific Conference on Power and Electrical Engineering of Riga Technical University, RTUCON 2014, Riga, Latvia, 14 October 2014; pp. 38–42. [[CrossRef](#)]
88. Chen, H.-C. Single-Loop Current Sensorless Control for Single-Phase Boost-Type SMR. *IEEE Trans. Power Electron.* **2009**, *24*, 163–171. [[CrossRef](#)]
89. Azcondo, F.J.; De Castro, A.; López, V.M.; García, O. Power factor correction without current sensor based on digital current rebuilding. *IEEE Trans. Power Electron.* **2010**, *25*, 1527–1536. [[CrossRef](#)]
90. Jeong, Y.-S.; Lee, S.-H.; Jeong, S.-G.; Kwon, J.-M.; Kwon, B.-H. High-Efficiency Bidirectional Grid-Tied Converter Using Single Power Conversion with High-Quality Grid Current. *IEEE Trans. Ind. Electron.* **2017**, *64*, 8504–8513. [[CrossRef](#)]